

Non-local Coulomb interaction and correlated electronic structure of TaS₂: A GW+EDMFT study

Taek Jung Kim, Min Yong Jeong, and Myung Joon Han

Department of Physics, Korea Advanced Institute of Science and Technology (KAIST), Daejeon 34141, Republic of Korea

E-mail: mj.han@kaist.ac.kr

Abstract. By means of *ab initio* computation schemes, we examine the low-energy electronic structure of monolayer TaS₂ in its low-temperature commensurate charge-density-wave structure. We estimate and take into account both local and non-local Coulomb correlations within cRPA (constrained random phase approximation) and GW+EDMFT (GW plus extended dynamical mean-field theory) method. Mott nature of its insulating phase is clearly identified. By increasing the level of nonlocal approximation from DMFT ($V = 0$) to EDMFT and GW+EDMFT, a systematic change of charge screening effects is clearly observed while its quantitative effect on the electronic structure is small in the realistic Mott state.

1. Introduction

Understanding the effect of Coulombic interaction between electrons in solid has long been a central theme of condensed matter physics [1, 2]. The relevant material systems are being extended to include various 2-dimensional (2D) van der Waals (vdW) materials [3–8] and more recently their twisted combinations [9–17]. The local onsite interaction (conventionally represented by U in Hubbard model) can induce electron localization, magnetic moment and thereby leading to metal-to-insulator and magnetic phase transition as well as other related phenomena such as unconventional superconductivity [1, 2, 18–20]. Non-local Coulomb interaction (denoted by V in extended Hubbard model) also plays an important role. Typically, it enhances the itinerancy of electrons by screening Coulomb interactions or broadening the effective bandwidth [21, 22]. Out of its competition with the local correlation, intersite interactions can cause the instability toward the charge-ordered phase or charge density wave (CDW) [21–26]. Recently, the effect of non-local Coulomb interaction receives increasing attentions in 2D material research [7, 27–30].

Among many correlated vdW materials, TaS₂ provides an intriguing case by displaying multiple quantum phases and their transitions [31–34]. At high temperature, TaS₂ is known to be metallic and has 1T structure shown in Fig. 1(a). As temperature is lowered, it exhibits so-called ‘nearly commensurate CDW (NCCDW)’, and then finally

becomes insulating [35, 36]. Superconductivity is also observed below $T_C \approx 2\text{--}5$ K by applying pressure, doping or electric field [31–33]. Importantly, the stabilization of the low temperature insulating phase is accompanied by commensurate CDW (CCDW) transition for which the long-range ‘star of David (SOD)’ pattern of atomic rearrangement is well identified in both experiments and simulations (see Fig. 2(a)) [35–39]. Therefore, unveiling the electronic property of CCDW SOD phase is important to understand the metal-insulator transition and the other related phases observed or suggested in this material at low temperature [31–34, 40–42]. Given that Ta atom has the 4+ formal valance, the SOD unit cell should have odd number of electrons (*i.e.*, $13 = 5d^1 \times 13$), and CCDW-TaS₂ is expected to be metallic according to the conventional band theory. It is however in a sharp contrast to experiments [43]. Several recent studies focusing this issue suggested Mott mechanism or interlayer dimerization to be responsible for metal-to-insulator transition [34, 44–50]. A crucially important challenge here is to estimate the strengths of Coulomb interactions [51].

Also related is another intriguing possibility in this material, namely quantum spin liquid (QSL) phase. Since the low-temperature CCDW phase makes a triangular lattice and carries nominally $S = 1/2$ local moment, the low temperature TaS₂ was suggested as a QSL candidate [40]. This idea is supported by the absence of long-range order down to very low temperatures and the gapless spin excitations [40–42]. Notably, a recent study highlighted the effect of non-local Coulomb interaction on the magnetic nature related to QSL [52]. However, most of previous computational studies on CCDW-TaS₂ have been limited to density functional theory (DFT), DFT+ U and single-site DMFT [44, 45, 53, 54], which is the main motivation of our current study.

In this paper, we examine the electronic structure and the effect of correlations in monolayer CCDW-TaS₂. First, we try to directly estimate the interaction strengths in terms of both U and V based on random phase approximation (RPA) [55–57]. The correlated electronic structure is calculated within GW+EDMFT (GW plus extended dynamical mean-field theory) [26, 58–60] which enables us to deal non-perturbatively with local and non-local Coulomb interaction. Our results show that monolayer TaS₂ is a Mott insulator mainly due to the local interaction. Even if the non-local Coulomb interaction is sizable, its effect on the electronic structure is quite small, largely suppressed in the Mott phase, and insufficient to achieve the charge-ordered phase.

2. Computational details

2.1. DFT and extended Hubbard model construction

We performed DFT calculations of monolayer 1T- and CCDW-TaS₂ with Vienna Ab initio Simulation Package (VASP) [61, 62]. The cell parameters and the internal coordinates were optimized with the force criterion of 0.1 meV/Å. The GGA-PBE functional [63] was used and the 25Å vacuum taken into account to simulate the monolayer. $21 \times 21 \times 1$ ($8 \times 8 \times 1$) k-grid and 500 eV (400 eV) cutoff energy were

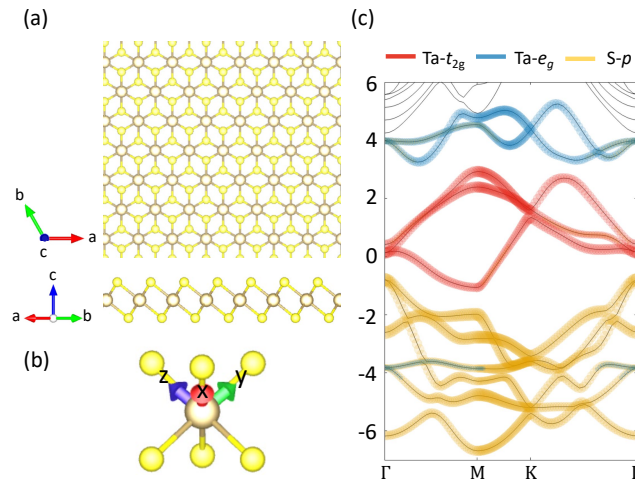


Figure 1. (a) Crystal structure of monolayer 1T-TaS₂. The top and side views are presented above and below respectively. (b) The local axis for octahedral structure of 1T-TaS₂ structure. (c) Electronic structure of monolayer 1T-TaS₂. Blue and red colors show Ta-t_{2g}, Ta-e_g orbital contribution in the rotated local axis of the octahedral structure respectively, and yellow shows the p orbital contribution of S atoms.

adopted for 1T-TaS₂ (CCDW-TaS₂).

To describe the effect of electronic correlations of low-energy state in CCDW-TaS₂, we consider the single-band extended Hubbard model:

$$H = - \sum_{ij\sigma} t_{ij} c_{i\sigma}^\dagger c_{j\sigma} + U \sum_i n_{i\uparrow} n_{i\downarrow} + V \sum_{\langle ij \rangle} n_i n_j - \mu \sum_i n_i \quad (1)$$

where $c_{i\sigma}^\dagger$ and $c_{i\sigma}$ is the creation and annihilation operator of electron, respectively, with spin $\sigma = \{\uparrow, \downarrow\}$ at site i . $n_i = c_{i\sigma}^\dagger c_{i\sigma}$ is electron number operator at site i , and $\sum_{\langle ij \rangle}$ denotes the nearest-neighbor summation. The hopping amplitude t_{ij} between two site i and j was calculated with the maximally localized Wannier function (MLWF) method [64, 65]. U and V is the local and non-local Coulomb interaction, respectively. The realistic estimation of these two interaction parameters is one of the main issues of current study. For this purpose, we used (c)RPA method as implemented in RESPACK code [57].

2.2. GW+EDMFT

The Hamiltonian is solved within GW+EDMFT whose standard self-consistent loop is briefly summarized below for the completeness of presentation [21, 26].

- (i) Calculate the lattice green function G and the screened Coulomb interaction W :

$$G(\mathbf{k}, i\omega_n) = [i\omega_n - t(\mathbf{k}) + \mu - \Sigma(\mathbf{k}, i\omega_n)]^{-1},$$

$$W(\mathbf{q}, i\Omega_m) = v(\mathbf{q})[1 - v(\mathbf{q})P(\mathbf{q}, i\Omega_m)]^{-1},$$

where \mathbf{k} and \mathbf{q} are the crystal momentum vectors. $i\omega_n$ and $i\Omega_m$ refers to the fermionic and bosonic Matsubara frequency, respectively. The momentum space

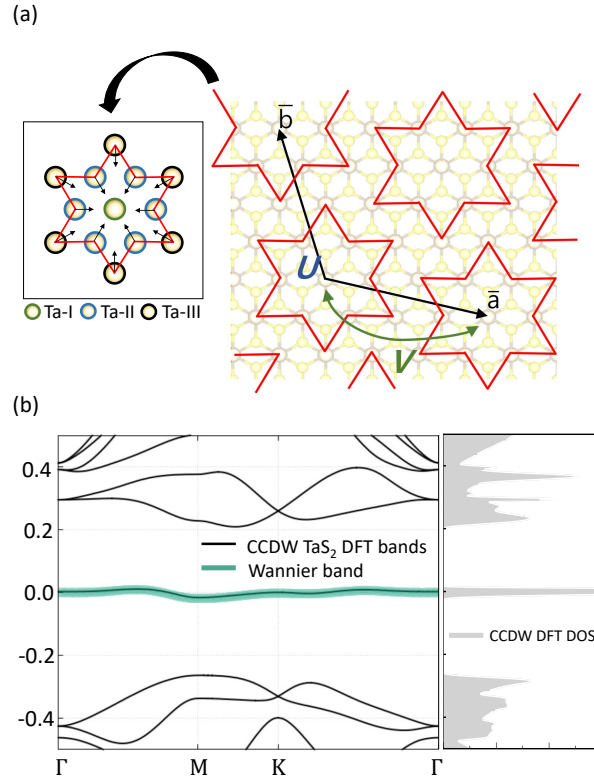


Figure 2. (a) Crystal structure of CCDW phase of TaS₂. Twelve Ta atoms move towards the central Ta constructing a unit of SOD and forming a single molecular orbital at the center. U and V refers to the onsite and the intersite Coulomb interaction of the molecular orbital, respectively. \bar{a} and \bar{b} are the unit cell vectors corresponding to CCDW phase. (b) The calculated DFT electronic structure for CCDW structure.

$t(\mathbf{k})$ corresponds to the Fourier transformed t_{ij} . $\Sigma(\mathbf{k}, i\omega_n)$ and $P(\mathbf{q}, i\Omega_m)$ represents the electron self-energy and the polarization function, respectively. The bare Coulomb interaction $v(\mathbf{q})$ is given by $v(\mathbf{q}) = 2V[\cos(q_x) + \cos(\frac{1}{2}q_x + \frac{\sqrt{3}}{2}q_y) + \cos(-\frac{1}{2}q_x + \frac{\sqrt{3}}{2}q_y)]$. In practice, we start the first loop from $\Sigma(\mathbf{k}, i\omega_n) = P(\mathbf{q}, i\Omega_m) = 0$.

(ii) Compute the fermionic and bosonic Weiss fields \mathcal{G} and \mathcal{U} :

$$\begin{aligned}\mathcal{G}(i\omega_n) &= [G_{\text{loc}}(i\omega_n) + \Sigma_{\text{loc}}(i\omega_n)]^{-1}, \\ \mathcal{U}(i\Omega_m) &= [W_{\text{loc}}(i\omega_n) + P_{\text{loc}}(i\Omega_m)]^{-1},\end{aligned}$$

where $A_{\text{loc}}(i\omega_n) = \sum_{\mathbf{k}} A(\mathbf{k}, i\omega_n)$ for any A .

(iii) Solve the following impurity model to obtain the impurity self-energy $\Sigma_{\text{imp}}(i\omega_n)$ and polarization $P_{\text{imp}}(i\Omega_m)$:

$$S_{\text{imp}} = \int \int_0^\beta d\tau d\tau' \bar{c}(\tau) [-\mathcal{G}^{-1}(\tau - \tau')] c(\tau') + \frac{1}{2} \int \int_0^\beta d\tau d\tau' \mathcal{U}(\tau - \tau') n(\tau) n(\tau')$$

where $A(\tau)$ is the fourier transformation of $A(i\omega_n)$, and $\bar{c}(\tau)$ and $c(\tau)$ are the Grassmann field for electrons. Here we took the continuous-time hybridization

expansion quantum Monte Carlo impurity solver as implemented in ComDMFT package [66].

- (iv) Construct the new self-energy and polarization function from the calculated $\Sigma_{\text{imp}}(i\omega_n)$ and $P_{\text{imp}}(i\Omega_m)$:

$$\begin{aligned}\Sigma(\mathbf{k}, i\omega_n) &= \Sigma_{\text{imp}}(i\omega_n) + \Sigma_{\text{nonloc}}^{\text{GW}}(\mathbf{k}, i\omega_n), \\ P(\mathbf{q}, i\Omega_m) &= P_{\text{imp}}(i\Omega_m) + P_{\text{nonloc}}^{\text{GW}}(\mathbf{q}, i\Omega_m),\end{aligned}$$

where $\Sigma^{\text{GW}}(\mathbf{k}, i\omega_n) = -\sum_{\mathbf{q}, i\Omega_m} G(\mathbf{k} + \mathbf{q}, i\omega_n + i\Omega_m)W(\mathbf{q}, i\Omega_m)$, $P^{\text{GW}}(\mathbf{q}, i\Omega_m) = 2\sum_{\mathbf{k}, i\omega_n} G(\mathbf{k} + \mathbf{q}, i\omega_n + i\Omega_m)G(\mathbf{k}, i\omega_n)$, and $A_{\text{nonloc}}(\mathbf{k}, i\omega_n) = A(\mathbf{k}, i\omega_n) - A_{\text{loc}}(i\omega_n)$.

- (v) Go back to the step (i) and repeat the calculations until $G(\mathbf{k}, i\omega_n)$ and $W(\mathbf{q}, i\Omega_m)$ are converged.

2.3. Coulomb interaction parameters

The direct first-principles calculation of interaction parameters corresponding to the low-energy CCDW molecular orbital is challenging due to the enlarged unitcell size (see Fig. 2). Therefore, previous studies of TaS₂ and NbSe₂ extracted the U values from the undistorted 1T-structure [44, 67]. Here we adopted the same approach of these two papers. In the sense that our calculation is based on (c)RPA, it is very similar with Ref. 67. In addition, we adopted two different approaches and also calculated the intersite interaction V which has not been reported before.

In Ref. 67, the U value corresponding to CCDW-NbSe₂ was estimated as the average of RPA-screened Coulomb interactions of Nb atoms in 1T-NbSe₂. We adopt it as our first way of calculating interaction parameter for CCDW-TaS₂:

$$U = \frac{1}{13^2} \sum_{\mathbf{R}, \mathbf{R}' \in \star} U_{\mathbf{R}-\mathbf{R}'} \quad (2)$$

where $U_{\mathbf{R}-\mathbf{R}'}$ is the Fourier transformed leading eigenvalue of RPA-screened Coulomb matrix $\mathcal{W}_{\mathbf{q}}^{\text{RPA}}$ represented in the eigenbasis of bare Coulomb matrix [67]. Here we calculated the screened Coulomb matrix for the t_{2g} states, namely, the red-colored bands shown in Fig. 1(c). \mathbf{R} and \mathbf{R}' are the lattice cell vectors corresponding to 1T structure, and \mathbf{q} is the lattice momentum. The white star symbol \star represents the indices of Ta atoms in the same SOD (which is composed of 13 Ta atoms; see Fig. 2(a)).

We take this idea of Ref. 67 and extend it to compute the intersite interaction:

$$V = \frac{1}{13^2} \sum_{\mathbf{R} \in \star, \mathbf{R}' \in \blackstar} U_{\mathbf{R}-\mathbf{R}'}. \quad (3)$$

Here the black star symbol \blackstar refers to the indices of Ta atoms belonging to the nearest-neighbor SOD (indicated by unit cell vector \bar{a} or \bar{b} ...; see Fig. 2(a)). The calculated U and V are presented in Table 1 which will be referred to as ‘3 bands RPA’ results hereafter.

Table 1. The calculated onsite (U) and intersite Coulomb interaction (V) for the molecular orbital of SOD charge density wave phase. The parameters are estimated from two different approaches, namely RPA and cRPA, as discussed in the main text.

	TaS ₂			NbSe ₂
	3 bands (RPA)	5 bands (cRPA)	Linear response	3bands (RPA)
U (eV)	0.371	0.653	0.180 [44]	0.300 [67]
V (eV)	0.208	0.359	-	-

Another possible way of calculating Coulomb parameters is to consider the weights of Ta atoms and to project them onto the molecular orbital of CCDW. In Ref. 44, U for the molecular orbital was estimated from the atomic Ta- d value, \bar{U}^{LR} , obtained from the (so-called) linear response method suggested by Cococcioni et al.[68]. The Coulomb interaction is estimated by calculating the projected weights of the Ta- d orbitals ($|d_a\rangle$) with respect to CCDW molecular orbitals ($|\Psi\rangle$):

$$\frac{U}{\bar{U}^{\text{LR}}} = \sum_{a \in \text{Ta}} |\langle d_a | \Psi \rangle|^4, \quad (4)$$

where a is the Ta atom index and Ta atoms are classified into three types, namely, Ta-I, Ta-II and Ta-III; see the inset of Fig. 2(a). Our calculations give rise to $|\langle d_a | \Psi \rangle|^2 = 0.229, 0.064,$ and 0.035 for when Ta-I, Ta-II, and Ta-III, respectively, which are in good agreement with a previous study [44].

Once again we extend this idea to calculate both U and V :

$$U = \sum_{\mathbf{R}, \mathbf{R}' \in \text{Ta}} |\langle d_{\mathbf{R}} | \Psi \rangle|^2 |\langle d_{\mathbf{R}'} | \Psi \rangle|^2 \bar{U}_{\mathbf{R}-\mathbf{R}'}, \quad (5)$$

$$V = \sum_{\mathbf{R} \in \text{Ta}, \mathbf{R}' \in \text{Se}} |\langle d_{\mathbf{R}} | \Psi \rangle|^2 |\langle d_{\mathbf{R}'} | \Psi \rangle|^2 \bar{U}_{\mathbf{R}-\mathbf{R}'}. \quad (6)$$

The Coulomb interaction $\bar{U}_{\mathbf{R}-\mathbf{R}'}$ is calculated by cRPA method within 5-band model of 1T-TaS₂ ($t_{2g} + e_g$ bands; see Fig. 1(c)). The results are presented in Table 1 which will be denoted as ‘5 bands cRPA’.

3. Results and discussion

3.1. Non-interacting electronic structure

Fig. 1(a) and (b) shows the crystal structure of 1T-TaS₂ and the local TaS₆ unit, respectively. The corresponding DFT-GGA band dispersion ($U = V = 0$ eV) is presented in Fig. 1(c) with the projected orbital characters at the local coordinates as

defined in Fig. 1(b). The Ta- t_{2g} states dominate the near Fermi level (E_F) region with t_{2g}^1 configuration. The higher energy bands above +3 eV and below -1 eV are mainly composed of Ta- e_g and S- p character, respectively. These overall electronic features are all in good agreement with previous studies [45, 69–71].

By lowering temperature, 1T-TaS₂ is known to undergo CDW structural transitions. So-called nearly commensurate charge density wave (NCCDW) phase is stabilized below $T \approx 350$ K and followed by CCDW at $T \approx 180$ K [35–37]. Figure 2(a) depicts the CCDW structure, so-called SOD pattern, in which twelve Ta atoms move toward the central one forming a 13-Ta-atom unit cluster [35, 36, 72, 73]. In this phase, the band structure is also changed accordingly [44, 45, 74, 75]. As shown in Fig. 2(b), a well-separated single electron band is solely responsible for the low energy region near E_F while six bonding orbital states are fully occupied by twelve Ta- d electrons well below E_F . It is noted that the near E_F band is fairly flat and nondispersive which is therefore prone to metal-to-insulator transition when interactions come in to play [44, 45, 74, 75].

In order to perform GW+EDMFT calculations with both on-site (U) and inter-site (V) parameters (see the right pannel of Fig. 2(a)), we first construct the non-interacting Hamiltonian for CCDW-TaS₂ by means of MLWF method [64, 65]. As shown in Fig. 2(b), this procedure well captures the target low energy electronic band; see the thick-green line (Wannier state) in good agreement with the black one (DFT band). The calculated hopping parameters of the first and the second neighbor hopping is $|t_1| = 1.812$ and $|t_2| = 0.814$ meV, respectively, and they are in good agreement with previous calculations [52, 76]. Interestingly, the third neighbor hopping $|t_3| = 1.785$ meV is larger than $|t_2|$ and comparable with $|t_1|$ as recently reported also by Chen et al.[52].

3.2. Interaction parameters

The metallic band structure of DFT-GGA demonstrates that Hubbard-type correlation is indispensable for reproducing insulating gap [43]. In fact, previous studies show that both DFT+ U and single-site DMFT calculation give rise to the correct insulating state while the former also predicts the magnetic ground state [44, 45]. According to the Yu et al.’s DMFT calculation, Mott phase transition starts to occur at $U \sim 0.7$ eV in bulk TaS₂ [45]. The effect of non-local interaction, on the other hand, has not been taken into account so far targeting the monolayer.

The important first step to have the realistic correlated electronic structure is to estimate interaction strengths. For the T- or H-phase of transition metal dichalcogenides (TMDs), there have been several attempts to perform the direct estimations [3, 44, 77–81]. Due to the demanding computation cost, however, *ab initio* calculation of these parameters corresponding to SOD phase is challenging. Only available are a few indirect calculations just for on-site parameter U [44, 67] (see Table 1).

Here we, for the first time, directly calculate both U and V of CCDW-TaS₂ from first-principles method based on RPA/cRPA. As discussed in the previous Section, we

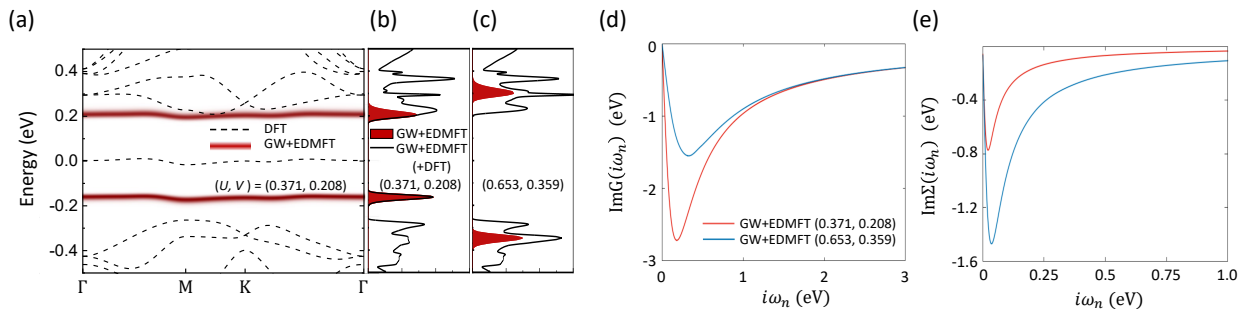


Figure 3. (a) The momentum-dependent spectral function of DFT (dashed lines) and GW+EDMFT (red line) calculated with Coulomb interactions estimated from 3 bands RPA model. The two numbers in parentheses indicate (U, V) in the unit of eV. (b-d) The calculated spectral function of GW+EDMFT with two different Coulomb interactions as estimated by (b) 3 bands RPA and (c) 5 bands cRPA model. The red colored data represent the density of states (DOS) of GW+EDMFT, and the black lines show the DFT DOS sum. (d) GW+EDMFT local self-energy computed by three different Coulomb parameter sets.

adopted two different approaches and the results are summarized in Table 1. The calculated U obtained from 3 bands RPA and 5 bands cRPA is 0.371 and 0.653 eV, respectively, both of which are notably larger than the result of a previous study based on linear response calculation [44].

It is interesting to compare the result of Ref. 44 with our 5 bands model both of which extract the interaction parameters by taking the projected weights of Ta- d orbitals onto CCDW-molecular orbitals. Interestingly, the on-site U for Ta- d (i.e., corresponding to the atomic on-site interaction) is larger in linear response calculation, $\bar{U}^{\text{LR}} = 2.27$ eV [44], than our cRPA $\bar{U}_{\mathbf{R}-\mathbf{R}'=\mathbf{0}} = 1.83$ eV. Given that the final result of U for CCDW phase is significantly larger in the 5 bands cRPA, the difference is not attributed to the discrepancy between cRPA and linear response method. Rather, it is clear from Eq. (5) that our projection method not just takes all of Eq. (4) portions into account but it also includes some inter-site contributions between different Ta atoms in a SOD molecular orbital.

Table 1 also shows that the calculated U for TaS₂ is larger than that for NbSe₂. As the computation method used by Kamil et al. [67] is based on 3 bands RPA, it is most straightforward to compare our result of $U=0.371$ eV (CCDW-TaS₂) with $U=0.300$ eV (CCDW-NbSe₂). According to a recent ARPES study by Nakata et al., the U value is smaller for NbSe₂ than TaSe₂ [82]. In addition, the value of TaSe₂ may be smaller than TaS₂ due to stronger screening by the chalcogen p -state [81, 83].

It is not surprising and but understandable to have different values of interaction parameters depending on the computation methods and details. For example, the weaker correlation in 3 bands RPA model than 5 bands cRPA is naturally attributed to the all screening channels taken into account in the former (namely, it is not *constrained*). Among the available results, one possible way of choice is to take the value that is in the best quantitative agreement with a particular experimental measurement. For example,

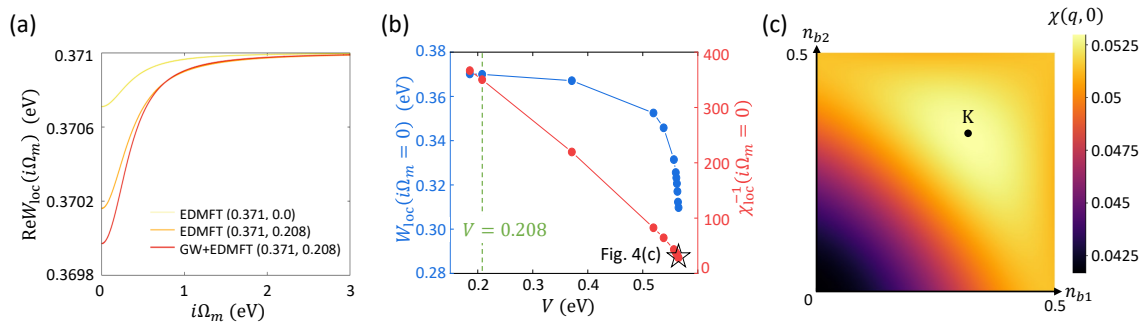


Figure 4. (a) The screened Coulomb interaction W calculated by DMFT (yellow), EDMFT (orange), and GW+EDMFT (red) methods. (b) The static part of $W(i\Omega_m = 0)$ (left y-axis) and $\chi_{\text{loc}}^{-1}(i\Omega_m = 0)$ (right y-axis) as a function of V . Our estimation of V value is indicated by vertical green-dotted line. The black star symbol indicates the value for Fig. (c). (c) The momentum-dependent charge susceptibility $\chi(\mathbf{q}, i\Omega_m = 0)$ in the vicinity of charge-ordered phase; computed at $(U, V) = (0.371 \text{ eV}, 0.565 \text{ eV})$

the gap size between the lower and upper Hubbard band has recently been measured by STM, and it gives rise to $U \sim 0.4 \text{ eV}$ [43]. Taking this experiment as the reference, our 3 bands model result provides the best quantitative agreement. For the sake of clarity, we will mainly present the result with this value in the remaining part of manuscript. However, it is obvious that all of our results coincidentally predict the large enough interaction strength with respect to the bandwidth $W \sim 9|t| \sim 0.02 \text{ eV}$.

3.3. GW+EDMFT results

Figure 3(a)–(c) summarize the GW+EDMFT results of spectral functions which were obtained by analytic continuation of Matsubara Green function using maximum entropy method [84]. In sharp contrast to the metallic DFT band structure, GW+EDMFT result clearly shows the insulating gap. From the local spectral function shown in Fig. 3(b), the upper and lower Hubbard peak is clearly observed at about $\pm 0.2 \text{ eV}$ which is in good agreement with a recent STM experiment of monolayer TaS₂ [43]. The result of 5 bands (cRPA) model is presented in Fig. 3(c). While this stronger correlation set of parameters also predicts the Mott insulating phase, the detailed electronic structure is noticeably different by positioning the Hubbard bands inside the uncorrelated states besides the enlarged gap size.

Figure 3(d) shows the imaginary part of local Green function calculated with two different parameter sets. It is clearly observed that $\text{Im}G(i\omega_n)$ goes to zero as $i\omega_n \rightarrow 0$, confirming the zero spectral weight of the insulating phase at E_F . The minimum frequency point is lower when the 3 bands RPA set is used $(U, V) = (0.371 \text{ eV}, 0.208 \text{ eV})$ than the 5 bands cRPA, reflecting the smaller gap size. The calculated self-energy is presented in Fig. 3(e). In both sets of parameters, the steep slope of $\partial \text{Im}\Sigma / \partial \omega_n$ at $i\omega_n \rightarrow 0$ also clearly indicates Mott phase; $Z = [1 - \frac{\partial \text{Im}\Sigma}{\partial \omega_n}]^{-1} \approx 0$.

Figure 4(a) shows the real part of screened Coulomb interaction. In order to examine the effect of non-local Coulomb interaction, we compare the three different

cases: With the fixed value of onsite interaction $U = 0.371$ eV, two different intersite interactions $V = 0$ and 0.208 eV have been considered together with GW self-energy. The frequency dependence shows that the effective Coulomb interaction approaches to the bare Coulomb $U = 0.371$ eV in the high-frequency limit, and decreases due to charge screenings in low frequency. It is noted that the low frequency part of W_{loc} gradually decreases as the more non-local interaction terms get involved. The same feature was also observed in the previous GW+EDMFT studies of the extended Hubbard model on a square lattice [21, 26]. Quantitatively, however, the screening by V is quite small. Namely, the charge fluctuation is largely suppressed in this Mott regime [21, 26]. In fact, the calculated $W(i\Omega_m = 0)$ is close to the value of $U = 0.371$ eV at around $V = 0.208$ eV; see the blue points on the green vertical dashed line in Fig. 4(b).

On the other hand, W is significantly reduced in the large V limit. It demonstrates that the charge fluctuations caused by V further screen the Coulomb interactions [21, 26]. In this regime of $V \gtrsim 0.5$ eV, W gets rapidly reduced, and simultaneously, the local charge susceptibility diverges (see the red points) [21, 26]:

$$\chi_{\text{loc}}^{-1} \rightarrow 0 \quad (7)$$

where $\chi_{\text{loc}} = \sum_{\mathbf{q}} \chi(\mathbf{q})$ and $\chi(\mathbf{q}) = \left(-P(\mathbf{q}, i\Omega_m)[1 - v(\mathbf{q})P(\mathbf{q}, i\Omega_m)]^{-1} \right)_{i\Omega_m=0}$. In Fig. 4(c), we plot the momentum-dependent static charge susceptibility at $V = 0.565$ eV (corresponding to the black star point in Fig. 4(b)). While the diverging feature at $(n_{b_1}, n_{b_2}) = (0, 333, 0, 333)$ indicates the charge-ordering instability (n_{b_i} is fractional coordinate of reciprocal lattice vector b_i), the largeness of V implies that it is unlikely in this system [21, 26].

When we were wrapping up the current work, a closely related paper was published [85] in which Chen et al. conducted GW+EDMFT calculations of triangular lattice. With a main emphasis on the comparison of two different GW+EDMFT computation schemes, they also investigated TaS₂. A notable difference is that they did not try to estimate the interaction parameters as well as hopping integrals from first-principles, but instead focused on the comparison to the experiment.

4. Summary

We investigated the electronic structure and the effect Coulomb interactions of monolayer TaS₂ with the combination of DFT, cRPA and GW+EDMFT. Both onsite and intersite correlation strengths are estimated based on two different *ab initio* cRPA approaches. The results coincidentally show that the monolayer CCDW-TaS₂ is in the Mott insulator regime. The comparison of DMFT, EDMFT and GW+EDMFT exhibits a systematic change of the electronic structure as the level of nonlocal self-energy computations are varied while its overall effect is small in terms of electronic structure. Our work provides useful information and insight for understanding TaS₂, other TMDC materials and the related systems.

5. Acknowledgment

T.J.K thanks Sangkook Choi for useful discussion of code implementations of GW+EDMFT, and Siheon Ryee for the useful tips on the convergence issues of GW+EDMFT. This work was supported by the National Research Foundation of Korea (NRF) grant funded by the Korea government (MSIT) (Grant Nos.2021R1A2C1009303 and NRF-2018M3D1A1058754).

References

- [1] Imada M, Fujimori A and Tokura Y 1998 *Rev. Mod. Phys.* **70** 1039–1263 publisher: American Physical Society URL <https://link.aps.org/doi/10.1103/RevModPhys.70.1039>
- [2] Lee P A, Nagaosa N and Wen X G 2006 *Rev. Mod. Phys.* **78** 17–85 publisher: American Physical Society URL <https://link.aps.org/doi/10.1103/RevModPhys.78.17>
- [3] van Loon E G C P, Rösner M, Schönhoff G, Katsnelson M I and Wehling T O 2018 *npj Quant Mater* **3** 1–8 ISSN 2397-4648 number: 1 Publisher: Nature Publishing Group URL <https://www.nature.com/articles/s41535-018-0105-4>
- [4] Zhang Y, Lu H, Zhu X, Tan S, Feng W, Liu Q, Zhang W, Chen Q, Liu Y, Luo X, Xie D, Luo L, Zhang Z and Lai X 2018 *Sci. Adv.* **4** eaao6791 ISSN 2375-2548 URL <https://www.science.org/doi/10.1126/sciadv.aao6791>
- [5] Kim H S, Haule K and Vanderbilt D 2019 *Phys. Rev. Lett.* **123** 236401 publisher: American Physical Society URL <https://link.aps.org/doi/10.1103/PhysRevLett.123.236401>
- [6] Kang S, Kim K, Kim B H, Kim J, Sim K I, Lee J U, Lee S, Park K, Yun S, Kim T, Nag A, Walters A, Garcia-Fernandez M, Li J, Chapon L, Zhou K J, Son Y W, Kim J H, Cheong H and Park J G 2020 *Nature* **583** 785–789 ISSN 1476-4687 number: 7818 Publisher: Nature Publishing Group URL <https://www.nature.com/articles/s41586-020-2520-5>
- [7] van Loon E G C P, Schüler M, Springer D, Sangiovanni G, Tomczak J M and Wehling T O 2020 *arXiv:2001.01735 [cond-mat]* ArXiv: 2001.01735 URL <http://arxiv.org/abs/2001.01735>
- [8] Vaño V, Amini M, Ganguli S C, Chen G, Lado J L, Kezilebieke S and Liljeroth P 2021 *Nature* **599** 582–586 ISSN 1476-4687 number: 7886 Publisher: Nature Publishing Group URL <https://www.nature.com/articles/s41586-021-04021-0>
- [9] Cao Y, Fatemi V, Demir A, Fang S, Tomarken S L, Luo J Y, Sanchez-Yamagishi J D, Watanabe K, Taniguchi T, Kaxiras E, Ashoori R C and Jarillo-Herrero P 2018 *Nature* **556** 80–84 ISSN 1476-4687 number: 7699 Publisher: Nature Publishing Group URL <https://www.nature.com/articles/nature26154>

- [10] Cao Y, Fatemi V, Fang S, Watanabe K, Taniguchi T, Kaxiras E and Jarillo-Herrero P 2018 *Nature* **556** 43–50 ISSN 1476-4687 number: 7699 Publisher: Nature Publishing Group URL <https://www.nature.com/articles/nature26160>
- [11] Yankowitz M, Chen S, Polshyn H, Zhang Y, Watanabe K, Taniguchi T, Graf D, Young A F and Dean C R 2019 *Science* **363** 1059–1064 ISSN 0036-8075, 1095-9203 URL <https://www.science.org/doi/10.1126/science.aav1910>
- [12] Burg G W, Zhu J, Taniguchi T, Watanabe K, MacDonald A H and Tutuc E 2019 *Phys. Rev. Lett.* **123** 197702 publisher: American Physical Society URL <https://link.aps.org/doi/10.1103/PhysRevLett.123.197702>
- [13] Liu X, Hao Z, Khalaf E, Lee J Y, Ronen Y, Yoo H, Haei Najafabadi D, Watanabe K, Taniguchi T, Vishwanath A and Kim P 2020 *Nature* **583** 221–225 ISSN 1476-4687 number: 7815 Publisher: Nature Publishing Group URL <https://www.nature.com/articles/s41586-020-2458-7>
- [14] Shen C, Chu Y, Wu Q, Li N, Wang S, Zhao Y, Tang J, Liu J, Tian J, Watanabe K, Taniguchi T, Yang R, Meng Z Y, Shi D, Yazyev O V and Zhang G 2020 *Nat. Phys.* **16** 520–525 ISSN 1745-2481 number: 5 Publisher: Nature Publishing Group URL <https://www.nature.com/articles/s41567-020-0825-9>
- [15] Cao Y, Rodan-Legrain D, Rubies-Bigorda O, Park J M, Watanabe K, Taniguchi T and Jarillo-Herrero P 2020 *Nature* **583** 215–220 ISSN 1476-4687 number: 7815 Publisher: Nature Publishing Group URL <https://www.nature.com/articles/s41586-020-2260-6>
- [16] Wang L, Shih E M, Ghiotto A, Xian L, Rhodes D A, Tan C, Claassen M, Kennes D M, Bai Y, Kim B, Watanabe K, Taniguchi T, Zhu X, Hone J, Rubio A, Pasupathy A N and Dean C R 2020 *Nat. Mater.* **19** 861–866 ISSN 1476-4660 number: 8 Publisher: Nature Publishing Group URL <https://www.nature.com/articles/s41563-020-0708-6>
- [17] Xu S, Al Ezzi M M, Balakrishnan N, Garcia-Ruiz A, Tsim B, Mullan C, Barrier J, Xin N, Piot B A, Taniguchi T, Watanabe K, Carvalho A, Mishchenko A, Geim A K, Fal’ko V I, Adam S, Neto A H C, Novoselov K S and Shi Y 2021 *Nat. Phys.* **17** 619–626 ISSN 1745-2481 number: 5 Publisher: Nature Publishing Group URL <https://www.nature.com/articles/s41567-021-01172-9>
- [18] Dagotto E 1994 *Rev. Mod. Phys.* **66** 763–840 publisher: American Physical Society URL <https://link.aps.org/doi/10.1103/RevModPhys.66.763>
- [19] Dagotto E 2005 *Science* **309** 257–262 publisher: American Association for the Advancement of Science URL <https://www.science.org/doi/10.1126/science.1107559>
- [20] Scalapino D J 2012 *Rev. Mod. Phys.* **84** 1383–1417 publisher: American Physical Society URL <https://link.aps.org/doi/10.1103/RevModPhys.84.1383>
- [21] Ayrat T, Biermann S, Werner P and Boehnke L 2017 *Phys. Rev. B* **95** 245130

- publisher: American Physical Society URL <https://link.aps.org/doi/10.1103/PhysRevB.95.245130>
- [22] Veld Y i t, Schüler M, Wehling T O, Katsnelson M I and Loon E G C P v 2019 *J. Phys.: Condens. Matter* **31** 465603 ISSN 0953-8984 publisher: IOP Publishing URL <https://doi.org/10.1088/1361-648x/ab36fe>
- [23] Wigner E 1934 *Phys. Rev.* **46** 1002–1011 publisher: American Physical Society URL <https://link.aps.org/doi/10.1103/PhysRev.46.1002>
- [24] Wigner E 1938 *Trans. Faraday Soc.* **34** 678–685 ISSN 0014-7672 publisher: The Royal Society of Chemistry URL <https://pubs.rsc.org/en/content/articlelanding/1938/tf/tf9383400678>
- [25] Lee P A and Fukuyama H 1978 *Phys. Rev. B* **17** 542–548 publisher: American Physical Society URL <https://link.aps.org/doi/10.1103/PhysRevB.17.542>
- [26] Ayral T, Biermann S and Werner P 2013 *Phys. Rev. B* **87** 125149 ISSN 1098-0121, 1550-235X URL <https://link.aps.org/doi/10.1103/PhysRevB.87.125149>
- [27] Rösner M, Steinke C, Lorke M, Gies C, Jahnke F and Wehling T O 2016 *Nano Lett.* **16** 2322–2327 ISSN 1530-6984 publisher: American Chemical Society URL <https://doi.org/10.1021/acs.nanolett.5b05009>
- [28] Raja A, Chaves A, Yu J, Arefe G, Hill H M, Rigosi A F, Berkelbach T C, Nagler P, Schüller C, Korn T, Nuckolls C, Hone J, Brus L E, Heinz T F, Reichman D R and Chernikov A 2017 *Nat Commun* **8** 15251 ISSN 2041-1723 number: 1 Publisher: Nature Publishing Group URL <https://www.nature.com/articles/ncomms15251>
- [29] Steinhoff A, Florian M, Rösner M, Schönhoff G, Wehling T O and Jahnke F 2017 *Nat Commun* **8** 1166 ISSN 2041-1723 number: 1 Publisher: Nature Publishing Group URL <https://www.nature.com/articles/s41467-017-01298-6>
- [30] Steinke C, Wehling T O and Rösner M 2020 *Phys. Rev. B* **102** 115111 publisher: American Physical Society URL <https://link.aps.org/doi/10.1103/PhysRevB.102.115111>
- [31] Sipos B, Kusmartseva A F, Akrap A, Berger H, Forró L and Tutiš E 2008 *Nature Mater* **7** 960–965 ISSN 1476-1122, 1476-4660 URL <http://www.nature.com/articles/nmat2318>
- [32] Ang R, Wang Z C, Chen C L, Tang J, Liu N, Liu Y, Lu W J, Sun Y P, Mori T and Ikuhara Y 2015 *Nat Commun* **6** 6091 ISSN 2041-1723 number: 1 Publisher: Nature Publishing Group URL <https://www.nature.com/articles/ncomms7091>
- [33] Yu Y, Yang F, Lu X F, Yan Y J, Cho Y H, Ma L, Niu X, Kim S, Son Y W, Feng D, Li S, Cheong S W, Chen X H and Zhang Y 2015 *Nature Nanotech* **10** 270–276 ISSN 1748-3395 number: 3 Publisher: Nature Publishing Group URL <https://www.nature.com/articles/nnano.2014.323>
- [34] Wang Y D, Yao W L, Xin Z M, Han T T, Wang Z G, Chen L, Cai C, Li Y and Zhang Y 2020 *Nat Commun* **11** 4215 ISSN 2041-1723 number: 1

- Publisher: Nature Publishing Group URL <https://www.nature.com/articles/s41467-020-18040-4>
- [35] Wilson J, Di Salvo F and Mahajan S 1975 *Advances in Physics* **24** 117–201 ISSN 0001-8732 publisher: Taylor & Francis eprint: <https://doi.org/10.1080/00018737500101391> URL <https://doi.org/10.1080/00018737500101391>
- [36] Fazekas P and Tosatti E 1979 *Philosophical Magazine B* **39** 229–244 ISSN 1364-2812 publisher: Taylor & Francis eprint: <https://doi.org/10.1080/13642817908245359> URL <https://doi.org/10.1080/13642817908245359>
- [37] Giambattista B, Slough C G, McNairy W W and Coleman R V 1990 *Phys. Rev. B* **41** 10082–10103 publisher: American Physical Society URL <https://link.aps.org/doi/10.1103/PhysRevB.41.10082>
- [38] Liu A Y 2009 *Phys. Rev. B* **79** 220515 publisher: American Physical Society URL <https://link.aps.org/doi/10.1103/PhysRevB.79.220515>
- [39] Ge Y and Liu A Y 2010 *Phys. Rev. B* **82** 155133 publisher: American Physical Society URL <https://link.aps.org/doi/10.1103/PhysRevB.82.155133>
- [40] Law K T and Lee P A 2017 *PNAS* **114** 6996–7000 ISSN 0027-8424, 1091-6490 publisher: National Academy of Sciences Section: Physical Sciences URL <https://www.pnas.org/content/114/27/6996>
- [41] Ribak A, Silber I, Baines C, Chashka K, Salman Z, Dagan Y and Kanigel A 2017 *Phys. Rev. B* **96** 195131 publisher: American Physical Society URL <https://link.aps.org/doi/10.1103/PhysRevB.96.195131>
- [42] Klanjšek M, Zorko A, Žitko R, Mravlje J, Jagličić Z, Biswas P, Prelovšek P, Mihailovic D and Arčon D 2017 *Nature Phys* **13** 1130–1134 ISSN 1745-2473, 1745-2481 URL <http://www.nature.com/articles/nphys4212>
- [43] Lin H, Huang W, Zhao K, Qiao S, Liu Z, Wu J, Chen X and Ji S H 2020 *Nano Res.* **13** 133–137 ISSN 1998-0124, 1998-0000 URL <http://link.springer.com/10.1007/s12274-019-2584-4>
- [44] Darancet P, Millis A J and Marianetti C A 2014 *Phys. Rev. B* **90** 045134 ISSN 1098-0121, 1550-235X URL <https://link.aps.org/doi/10.1103/PhysRevB.90.045134>
- [45] Yu X L, Liu D Y, Quan Y M, Wu J, Lin H Q, Chang K and Zou L J 2017 *Phys. Rev. B* **96** 125138 publisher: American Physical Society URL <https://link.aps.org/doi/10.1103/PhysRevB.96.125138>
- [46] Lee S H, Goh J S and Cho D 2019 *Phys. Rev. Lett.* **122** 106404 ISSN 0031-9007, 1079-7114 URL <https://link.aps.org/doi/10.1103/PhysRevLett.122.106404>
- [47] Petocchi F, Nicholson C W, Salzmänn B, Pasquier D, Yazyev O V, Monney C and Werner P 2022 *arXiv:2202.01285 [cond-mat]* ArXiv: 2202.01285 URL <http://arxiv.org/abs/2202.01285>

- [48] Butler C J, Yoshida M, Hanaguri T and Iwasa Y 2020 *Nat Commun* **11** 2477 ISSN 2041-1723 URL <http://www.nature.com/articles/s41467-020-16132-9>
- [49] Lee J, Jin K H and Yeom H W 2021 *Phys. Rev. Lett.* **126** 196405 publisher: American Physical Society URL <https://link.aps.org/doi/10.1103/PhysRevLett.126.196405>
- [50] Nicholson C W, Petocchi F, Salzmann B, Witteveen C, Rumo M, Kremer G, von Rohr F O, Werner P and Monney C 2022 *arXiv:2204.05598 [cond-mat]* ArXiv: 2204.05598 URL <http://arxiv.org/abs/2204.05598>
- [51] Fuhrmann A, Heilmann D and Monien H 2006 *Phys. Rev. B* **73** 245118 publisher: American Physical Society URL <https://link.aps.org/doi/10.1103/PhysRevB.73.245118>
- [52] Chen G, Rösner M and Lado J L 2022 *arXiv:2201.07826 [cond-mat]* ArXiv: 2201.07826 URL <http://arxiv.org/abs/2201.07826>
- [53] Yi S, Zhang Z and Cho J H 2018 *Phys. Rev. B* **97** 041413 ISSN 2469-9950, 2469-9969 URL <https://link.aps.org/doi/10.1103/PhysRevB.97.041413>
- [54] Jiang T, Hu T, Zhao G D, Li Y, Xu S, Liu C, Cui Y and Ren W 2021 *Phys. Rev. B* **104** 075147 publisher: American Physical Society URL <https://link.aps.org/doi/10.1103/PhysRevB.104.075147>
- [55] Aryasetiawan F, Imada M, Georges A, Kotliar G, Biermann S and Lichtenstein A I 2004 *Phys. Rev. B* **70** 195104 ISSN 1098-0121, 1550-235X URL <https://link.aps.org/doi/10.1103/PhysRevB.70.195104>
- [56] Şaşoğlu E, Friedrich C and Blügel S 2011 *Phys. Rev. B* **83** 121101 ISSN 1098-0121, 1550-235X URL <https://link.aps.org/doi/10.1103/PhysRevB.83.121101>
- [57] Nakamura K, Yoshimoto Y, Nomura Y, Tadano T, Kawamura M, Kosugi T, Yoshimi K, Misawa T and Motoyama Y 2021 *Computer Physics Communications* **261** 107781 ISSN 0010-4655 URL <https://www.sciencedirect.com/science/article/pii/S001046552030391X>
- [58] Sun P and Kotliar G 2002 *Phys. Rev. B* **66** 085120 publisher: American Physical Society URL <https://link.aps.org/doi/10.1103/PhysRevB.66.085120>
- [59] Biermann S, Aryasetiawan F and Georges A 2003 *Phys. Rev. Lett.* **90** 086402 ISSN 0031-9007, 1079-7114 URL <https://link.aps.org/doi/10.1103/PhysRevLett.90.086402>
- [60] Sun P and Kotliar G 2004 *Phys. Rev. Lett.* **92** 196402 ISSN 0031-9007, 1079-7114 URL <https://link.aps.org/doi/10.1103/PhysRevLett.92.196402>
- [61] Kresse G and Hafner J 1993 *Phys. Rev. B* **48** 13115–13118 URL <https://link.aps.org/doi/10.1103/PhysRevB.48.13115>
- [62] Kresse G and Furthmüller J 1996 *Comput. Mater. Sci.* **6** 15–50 ISSN 0927-0256 URL <http://www.sciencedirect.com/science/article/pii/S0927025696000080>

- [63] Perdew J P, Burke K and Ernzerhof M 1996 *Phys. Rev. Lett.* **77** 3865–3868 URL <https://link.aps.org/doi/10.1103/PhysRevLett.77.3865>
- [64] Marzari N and Vanderbilt D 1997 *Phys. Rev. B* **56** 12847–12865 URL <https://link.aps.org/doi/10.1103/PhysRevB.56.12847>
- [65] Souza I, Marzari N and Vanderbilt D 2001 *Phys. Rev. B* **65** 035109 URL <https://link.aps.org/doi/10.1103/PhysRevB.65.035109>
- [66] Choi S, Semon P, Kang B, Kutepov A and Kotliar G 2019 *Computer Physics Communications* **244** 277–294 ISSN 0010-4655 URL <https://www.sciencedirect.com/science/article/pii/S0010465519302140>
- [67] Kamil E, Berges J, Schönhoff G, Rösner M, Schüler M, Sangiovanni G and Wehling T O 2018 *J. Phys.: Condens. Matter* **30** 325601 ISSN 0953-8984, 1361-648X URL <https://iopscience.iop.org/article/10.1088/1361-648X/aad215>
- [68] Cococcioni M 2005 *Phys. Rev. B* **71**
- [69] Mattheiss L F 1973 *Phys. Rev. B* **8** 3719–3740 publisher: American Physical Society URL <https://link.aps.org/doi/10.1103/PhysRevB.8.3719>
- [70] Smith N V, Kevan S D and DiSalvo F J 1985 *J. Phys. C: Solid State Phys.* **18** 3175–3189 ISSN 0022-3719 publisher: IOP Publishing URL <https://doi.org/10.1088/0022-3719/18/16/013>
- [71] Yan-Bin Q, Yan-Ling L, Guo-Hua Z, Zhi Z and Xiao-Ying Q 2007 *Chinese Phys.* **16** 3809–3814 ISSN 1009-1963 publisher: IOP Publishing URL <https://doi.org/10.1088/1009-1963/16/12/042>
- [72] Tosatti E and Fazekas P 1976 *J. Phys. Colloques* **37** C4–168 ISSN 0449-1947, 2777-3418 publisher: EDP Sciences URL <http://dx.doi.org/10.1051/jphyscol:1976426>
- [73] Brouwer R and Jellinek F 1980 *Physica B+C* **99** 51–55 ISSN 0378-4363 URL <https://www.sciencedirect.com/science/article/pii/0378436380902090>
- [74] Perfetti L, Georges A, Florens S, Biermann S, Mitrovic S, Berger H, Tomm Y, Höchst H and Grioni M 2003 *Phys. Rev. Lett.* **90** 166401 publisher: American Physical Society URL <https://link.aps.org/doi/10.1103/PhysRevLett.90.166401>
- [75] Perfetti L, Loukakos P A, Lisowski M, Bovensiepen U, Berger H, Biermann S, Cornaglia P S, Georges A and Wolf M 2006 *Phys. Rev. Lett.* **97** 067402 publisher: American Physical Society URL <https://link.aps.org/doi/10.1103/PhysRevLett.97.067402>
- [76] Pasquier D and Yazyev O V 2022 *Phys. Rev. B* **105** L081106 publisher: American Physical Society URL <https://link.aps.org/doi/10.1103/PhysRevB.105.L081106>
- [77] Hüser F, Olsen T and Thygesen K S 2013 *Phys. Rev. B* **88** 245309 publisher: American Physical Society URL <https://link.aps.org/doi/10.1103/PhysRevB.88.245309>

- [78] Ugeda M M, Bradley A J, Shi S F, da Jornada F H, Zhang Y, Qiu D Y, Ruan W, Mo S K, Hussain Z, Shen Z X, Wang F, Louie S G and Crommie M F 2014 *Nature Mater* **13** 1091–1095 ISSN 1476-4660 number: 12 Publisher: Nature Publishing Group URL <https://www.nature.com/articles/nmat4061>
- [79] Kim T J, Ryee S, Han M J and Choi S 2020 *2D Mater.* **7** 035023 ISSN 2053-1583 publisher: IOP Publishing URL <https://doi.org/10.1088/2053-1583/ab8b48>
- [80] Boix-Constant C, Mañas-Valero S, Córdoba R, Baldoví J J, Rubio A and Coronado E 2021 *ACS Nano* **15** 11898–11907 ISSN 1936-0851 publisher: American Chemical Society URL <http://lps3.pubs.acs.org.libra.kaist.ac.kr/doi/10.1021/acsnano.1c03012>
- [81] Karbalaee Aghaee A, Belbasi S and Hadipour H 2022 *Phys. Rev. B* **105** 115115 publisher: American Physical Society URL <https://link.aps.org/doi/10.1103/PhysRevB.105.115115>
- [82] Nakata Y, Sugawara K, Chainani A, Oka H, Bao C, Zhou S, Chuang P Y, Cheng C M, Kawakami T, Saruta Y, Fukumura T, Zhou S, Takahashi T and Sato T 2021 *Nat Commun* **12** 5873 ISSN 2041-1723 number: 1 Publisher: Nature Publishing Group URL <https://www.nature.com/articles/s41467-021-26105-1>
- [83] Miyake T, Nakamura K, Arita R and Imada M 2010 *J. Phys. Soc. Jpn.* **79** 044705 ISSN 0031-9015 publisher: The Physical Society of Japan URL <https://journals.jps.jp/doi/abs/10.1143/JPSJ.79.044705>
- [84] Jarrell M and Gubernatis J 1996 *Phys. Rep.* **269** 133–195 ISSN 0370-1573
- [85] Chen J, Petocchi F and Werner P 2022 *Phys. Rev. B* **105** 085102 publisher: American Physical Society URL <https://link.aps.org/doi/10.1103/PhysRevB.105.085102>